Applied Physics A (2021) 127:665
https://doi.org/10.1007/s00339-021-04818-w

Applied Physics A
Materials Science & Processing

High-quality percussion drilling with ultrashort laser pulses

A. Feuer[1] · R. Weber[1] · R. Feuer[2] · D. Brinkmeier[1] · T. Graf[1]

Received: 14 June 2021 / Accepted: 26 July 2021 / Published online: 12 August 2021

Abstract
The influence of the laser fluence on the quality of percussion-drilled holes was investigated both experimentally and by an analytical model. The study reveals that the edge quality of the drilled microholes depends on the laser fluence reaching the rear exit of the hole and changes with the number of pulses applied after breakthrough. The minimum fluence that must reach the hole's exit in order to obtain high-quality microholes in stainless steel was experimentally found to be 2.8 times the ablation threshold.

Keywords Laser materials processing · Laser micro-drilling · Drilling model · Percussion drilling · Hole quality · Edge quality

1 Introduction

Percussion drilling is one of the most effortless laser applications to implement, as only a focusing lens is required to focus the laser beam on the workpiece. Micro-drilling with ultrashort laser pulses is, however, a highly dynamic process in which a multitude of mechanisms interact at high temperatures and pressures on very small temporal and spatial scales [1, 2]. At present, it is still a demanding task to separate and understand the many effects that occur during the drilling process. With the use of additional process strategies such as helical drilling [3–6], the use of process gas [3] and focus adjustment [7] as well as the availability of higher pulse energies of up to several millijoules [8, 9], not only the number of process parameters increases, but also the number of effects that occur. Thus, it is still challenging to reliably predict the drilling depth, borehole geometry, and drilling duration, especially with analytical models. An important step in this direction was to understand and describe the heat accumulation that occurs during machining with ultrashort laser pulses [10–13] and its consequences on the drilling process [14, 15]. When heat accumulation effects and particle-ignited plasmas can be avoided, it is possible to estimate the final depth of percussion-drilled microholes with an analytical model [16, 17] and the temporal evolution of the drilling depth can be predicted [18]. In the latter case, the use of optical coherence tomography (OCT) proved to be a promising diagnostic method to measure the drilling progress online.

For many high-tech applications, such as drilling of injection nozzles [19] or drilling of spinnerets for fibre production [4, 20], the quality of the microholes is of crucial importance. In particular, the quality of the edge and the shape accuracy of the microhole are relevant criteria. The quality-reducing effects that can occur during laser drilling are manifold and the impact of these effects include shape deviations, striations, burrs, side channels, and the formation of multiple holes. Although the studies published in [16] and [18] deal with the production of high-quality microholes, the classification of high-quality microholes primarily only refers to the exclusion of thermal damage and excessive melting due to heat accumulation. The quality of the microhole's edge on the side where the laser beam exits and its dependence on processing parameters was not investigated in these studies and is now addressed in the present work. From previously published work, it is already known that side channels form at the far end of the hole when the fluence reaching the tip is close to the ablation threshold [21]. Such side channels appear as multiple holes on the rear side of the workpiece, but can be avoided by increasing the incident laser fluence [17]. Both studies indicate that the fluence has a significant influence on the quality of the microhole's

✉ A. Feuer
anne.feuer@ifsw.uni-stuttgart.de

[1] Institut für Strahlwerkzeuge (IFSW), University of Stuttgart, Pfaffenwaldring 43, 70569 Stuttgart, Germany

[2] 73733 Esslingen, Germany

exit. The fluence reaching the far end of the hole changes with the evolving geometry of the hole being drilled [18]. As known from experiments, the same happens with the quality of the holes. A simplified analytical model is therefore proposed in the following to calculate the fluence reaching the microhole's exit. By comparison to experimental results, we show that the quality of the holes significantly deteriorates as soon as the fluence reaching the far end of the hole drops below a value of 2.8 times the ablation threshold of the material.

In the following, the experimental setup is presented in Sect. 2 together with the method applied to classify and determine the edge quality of the holes. The experimental investigations on the edge quality of the hole's exit are presented in Sect. 3, followed by the derivation of the analytical model for the calculation of the fluence at the hole's exit in Sect. 4. Finally, by correlating the experimental results to the theoretical calculations, the conditions under which high-quality exits can be produced are derived in Sect. 5.

2 Methods

2.1 Experimental setup

The experiments were performed using an ultrafast titan sapphire laser system (Spitfire ACE, Spectra Physics) operating at a wavelength λ of 800 nm. The laser system provides ultrashort laser pulses with an adjustable pulse duration τ from 35 fs to 5 ps and with pulse energies E_P of up to 7 mJ at a repetition rate f_R of 1 kHz. The pulse duration was set to 1 ps (FWHM, Gauss-fit). The circularly polarized Gaussian beam with a beam diameter of 3.7 mm ($1/e^2$ diameter) was focused by a telecentric f-theta lens with a focal length of 100 mm to a focal diameter of $d_f = 36$ µm ($1/e^2$ diameter). The beam quality factor was measured to be $M^2 = 1.3$. The focus was positioned 5 mm below the surface of the 0.5 mm thick workpiece made of cold-rolled stainless steel (St 1.4301/AISI 304). The beam diameter on the workpiece's surface thus was $d_s = 188$ µm. The diameters were measured using a beam profiling camera. A galvanometer scanner was used to position the laser beam on the workpiece. Both the pulse energy (and with it the fluence) incident on the workpiece and the number of pulses applied to a single drilled hole were varied in the experiments. To account for statistical variability, 10 holes were drilled with each set of parameters.

2.2 Analysis of the drilled holes

The edges of the exits of the microholes were quantitatively evaluated by automated analysis of microscope images. The microscope images used had a resolution of 0.3 µm/px. For the automated analysis, a supervised learning approach was used to reliably determine the contour shape of the hole's opening [22, 23]. The image analysis was performed with the software *Mathematica 12.1*. Figure 1 shows the microscope image of a microhole's exit (a) and the opening of the microhole identified by supervised learning (b). An ellipse was fitted to the determined contour of the hole's exit with the least squares method (see Fig. 1c). Figure 1d shows the radial deviation of the hole's edge from the fitted ellipse. Based on these data, the amplitude of striations ξ and the perimeter ratio σ can be determined, which are introduced in the following.

The striations are quantified based on the deviation of the hole's contour from the fitted ellipse. The distance between the 5% and 95% quantile of this deviation is used as a measure of the amplitude of the striations ξ (see Fig. 1d). The perimeter ratio σ is defined as the ratio between the length of the hole´s contour and the circumference of the fitted ellipse and thus is a measure of the frequentness of the striations. These two quantities allow to assess different edge qualities of microholes, as shown by the exemplary images in Fig. 2 used to define for four different quality types: ideal, round exit (a), exit with one larger striation (b), exit with many small striations (c), and exit with many larger striations (d). Only exits with both, a small ξ and a small σ, indicate that it is an exit with good edge quality.

3 Evolution of the edge quality during the drilling process

The evolution of the edge quality of the holes' exits during the drilling process is shown in Fig. 3 for microholes which were percussion drilled with a peak fluence of 8.6 J/cm^2 in a Gaussian beam. Figure 3 shows the striations amplitude ξ (a) and the perimeter ratio σ (c) as well as selected microscope images (b) of the exits of the microholes as a function of the total number of applied pulses. With the parameters used, the exits of the microholes after the breakthrough exhibit a high quality with an even, almost circular contour. Only if more than 10,000 pulses are applied, the edge quality deteriorates significantly and striations become clearly apparent on the wall and consequently shape the contour of the exit. Based on the parameters ξ and σ, the exits of the microholes can be assigned to two quality classes using a k-means clustering algorithm [24]. The range in which the applied number of pulses leads to exits with low values of ξ and σ, hence producing holes with high-quality exits, is marked in green. With the parameters used, the breakthrough was reached after about 5000 pulses. The width of the range leading to high-quality exits is $\Delta N_q = (5000 \pm 500)$ pulses after breakthrough.

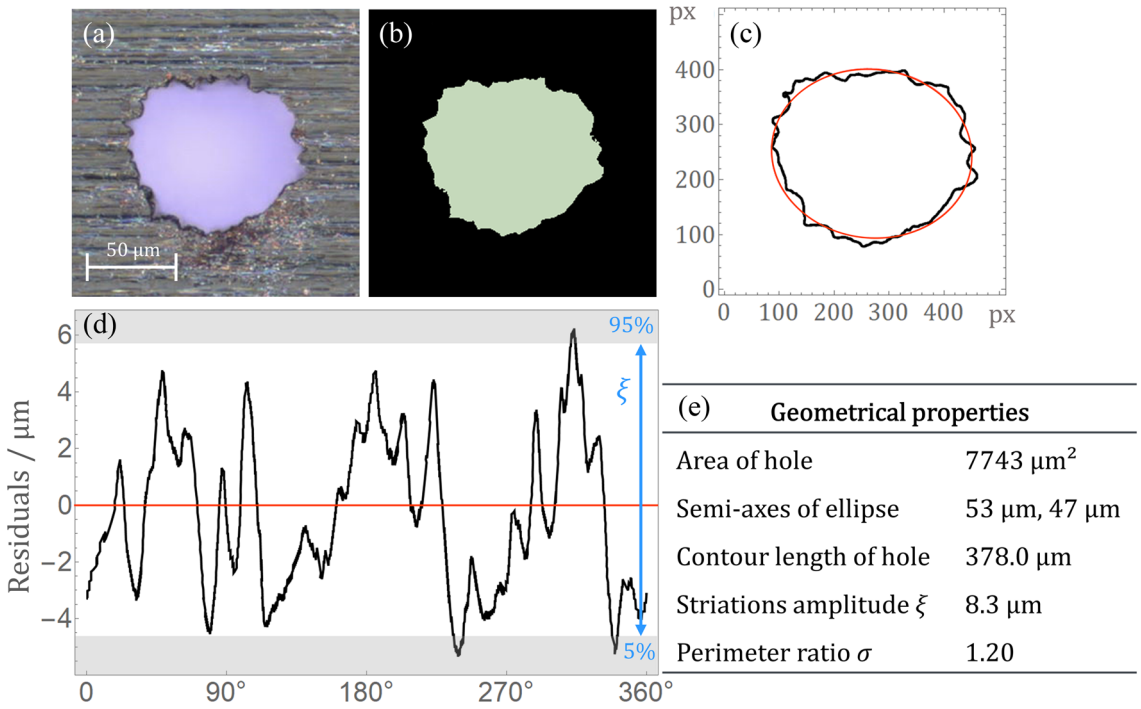

Fig. 1 Microscope image of a microhole's exit (**a**). Shape of the hole's exit as extracted by image processing (**b**). Ellipse (red) fitted to the determined contour of the hole's exit (**c**). The plot in **d** shows the radial deviation of the hole's edge from the fitted ellipse and the striations amplitude ξ. The geometrical properties of the hole's exit are summarized in (**e**)

Shapes	(a)	(b)	(c)	(d)
Striations amplitude ξ / px	1.3	38.4	9.7	46.6
Perimeter ratio σ / px	1.05	1.09	1.67	1.36

Fig. 2 Exemplary images (500 × 500 pixels) and geometrical properties for different types of edge quality: ideal, round exit (**a**), exit with one larger striation (**b**), exit with many small striations (**c**), and exit with many larger striations (**d**)

As seen from Fig. 4, this abrupt change of the quality can be observed also when drilling with other pulse energies. Thereby, it was found that the range in which exits of high quality are formed decreases with decreasing peak fluence to (4000 ± 500) pulses after breakthrough at 6.5 J/cm^2 and to (2000 ± 500) pulses after breakthrough at 4.3 J/cm^2, respectively. For microholes drilled at a further reduced fluence of 2.6 J/cm^2, no high-quality microholes were formed, hence $\Delta N_q = 0$ (data not shown).

The results show that high-quality exits are obtained only during the phase in which the diameter of the exits undergoes a significant widening rate. The development of the mid-range diameter of the exits and entrances of the drilled microholes is shown in Fig. 5. As expected from the model [18] presented in Sect. 4, the diameter of the entrances remains almost constant with increasing number of pulses. The evaluation of the quality of the entrances reveals that the entrances are always characterized by a high degree of striations throughout the entire drilling process (data not shown). The striations amplitude ξ and perimeter ratio σ for the entrances of the microholes generally lie in the range of $\xi = (21 \pm 5)$ µm and $\sigma = 1.48 \pm 0.1$ for all three fluences and are thus well above the values of the exits. The extent and location of the striations within the drilling channel can be seen in the two insets of Fig. 5, each showing the cross section of a microhole produced with a peak fluence of 8.6 J/

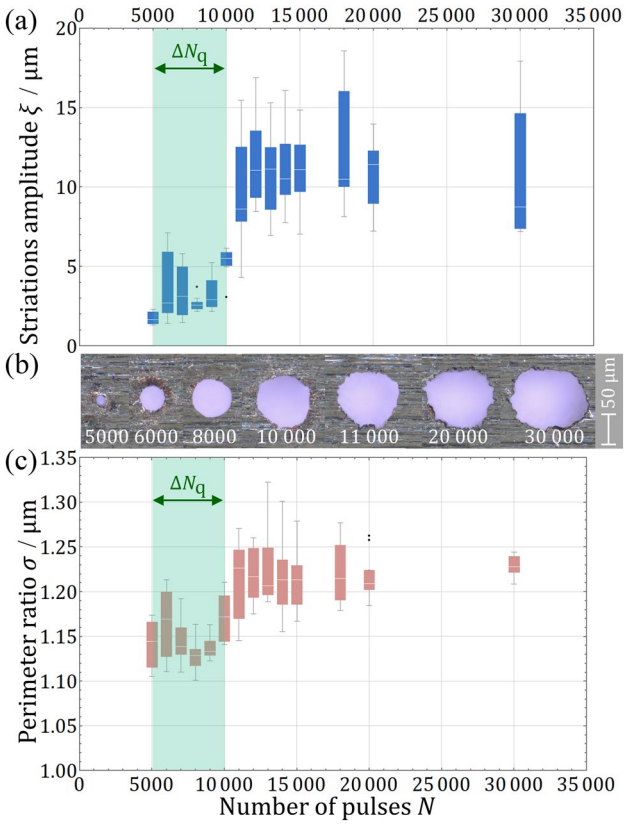

Fig. 3 Striations amplitude ξ (**a**), microscope images (**b**), **b** and perimeter ratio σ (**c**) of the microhole exits which were produced in 0.5 mm thick samples of stainless steel (St 1.4301/AISI 304) with different number of pulses with a peak fluence of 8.6 J/cm^2 in Gaussian beam ($\lambda = 800$ nm,$\tau = 1$ ps,$f_R = 1$ kHz,$E_P = 1.2$ mJ). The green section highlights the range ΔN_q after breakthrough in which high-quality exits are formed

cm^2. The microhole shown on the left was drilled with a total of 8000 pulses and thus lies within the quality range. In this case, striations are only present in the upper two thirds of the drilling channel. The microhole shown on the right was drilled with a total of 11,000 pulses and thus lies outside the quality range. Here, the striations already extend over the entire drilling channel and thus shape the microhole exit.

4 Analytical model of the fluence at the exit of percussion-drilled microholes

In the previous section, it was shown that the edge quality of the microhole's exit changes significantly during the drilling process. In particular, it has been observed that high-quality exits are formed immediately after the breakthrough and that the edge quality deteriorated only after an increased number of pulses by an intensified formation of striations. The experimental study also reveals that the range of the number of applied pulses after breakthrough, in which high-quality exits were maintained, decreases with decreasing peak fluence of the incident Gaussian beam. This may suggest the hypothesis that the abrupt deterioration of the edge quality at the upper end of this range could be caused when the fluence reaching the far exit of the holes drops below a certain limit. To investigate whether the fluence at the exit can explain a change of the edge quality, the following section presents an analytical estimation of the fluence reaching the exit of the microholes. Assuming that a minimum fluence at the microhole's exit is required to obtain edges of high quality, conditions can be derived under which high-quality microhole exits can be produced as later verified in Sect. 5.

4.1 Fluence at the microhole's exit

The fluence at the exit of the microhole can be derived from the analytical drilling model published in [18], which predicts the temporal evolution of the drilling depth of blind holes. The model assumes a conical shape of the evolving microhole, where z_{tip} is its depth and r_{entr} is the radius of the hole's entrance (see Fig. 6a, modified for the following discussion of through-holes). Assuming that the laser beam incident on the top of the workpiece has a Gaussian fluence distribution $\Phi(r) = \phi_0 \bullet \exp\left(-2r^2/w^2\right)$ the radius of the entrance of the drilled hole is given by [25, 26]

$$r_{entr} = w\sqrt{\frac{1}{2}\ln\left(\frac{A\phi_0}{\phi_{abs,th}}\right)}, \quad \Phi_0 \geq \Phi_{abs,th}/A, \tag{1}$$

where A is the material-specific absorptivity on the surface of the workpiece and

$$\phi_0 = 2E_P/\left(\pi w^2\right) \tag{2}$$

is the peak fluence on the workpiece in the centre of the Gaussian beam and w is the beam radius on the surface of the workpiece [27].

The distribution of the pulse energy E_P of the incident laser pulses on the inner walls of the microhole is influenced by multiple reflections. It was shown in [18] that a good agreement with experimental results is obtained with the assumption that the absorbed fluence increases linearly along the depth of the microhole starting from a value given by the ablation threshold fluence $\Phi_{abs,th}$ at the edge of the entrance to the value [18]

$$\Phi_{\eta,tip} = \frac{3\eta\left(1 - \frac{\phi_{abs,th}}{A\,\phi_0}\right)E_P}{A_{cone}} - 2\Phi_{abs,th}, \quad A_{cone} > 0, \tag{3}$$

at the tip of the blind microhole, where η is the integral absorptance of the hole,

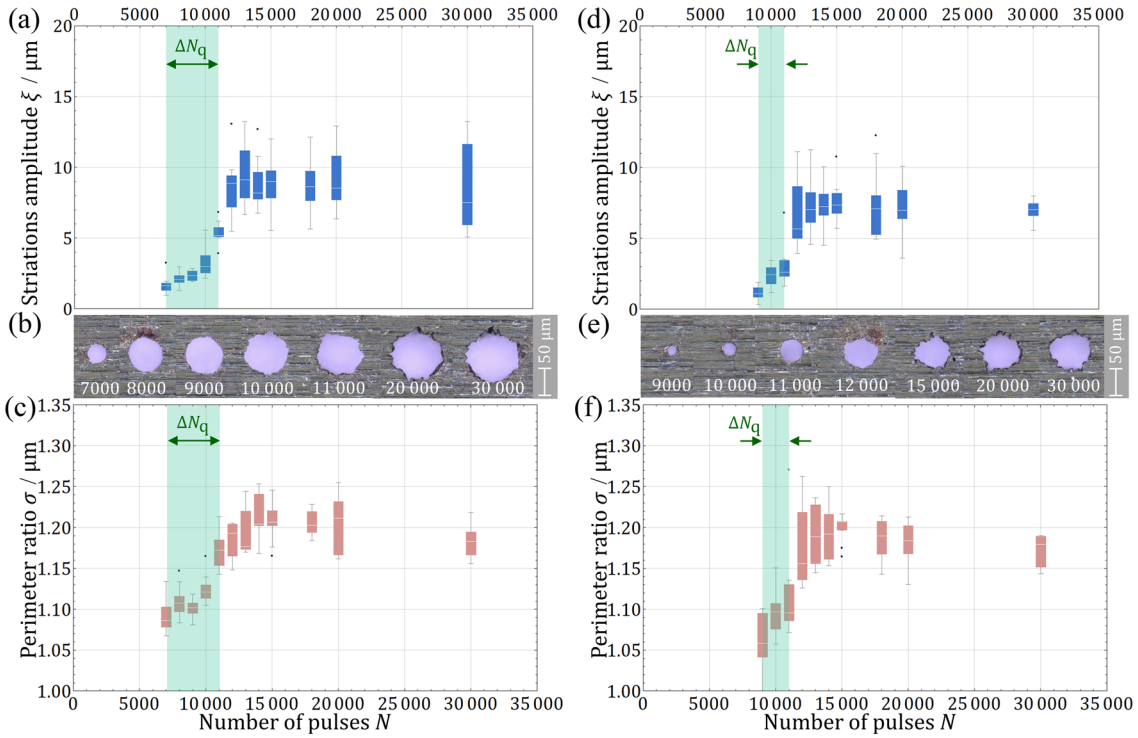

Fig. 4 Striations amplitude ξ (**a**, **d**), microscope images (**b**, **e**), and perimeter ratio σ (**c**, **f**) of the exits of microholes which were produced in 0.5 mm thick samples of stainless steel (St 1.4301/AISI 304) with a peak fluence of 6.5 J/cm^2 (left) and 4.3 J/cm^2 (right) in Gaussian beam ($\lambda = 800$ nm,$\tau = 1$ ps,$f_R = 1$ kHz,$E_P = 0.9$ mJ (left) and $E_P = 0.6$ mJ (right)). The green section highlights the range of pulse numbers ΔN_q after breakthrough in which high-quality exits are formed

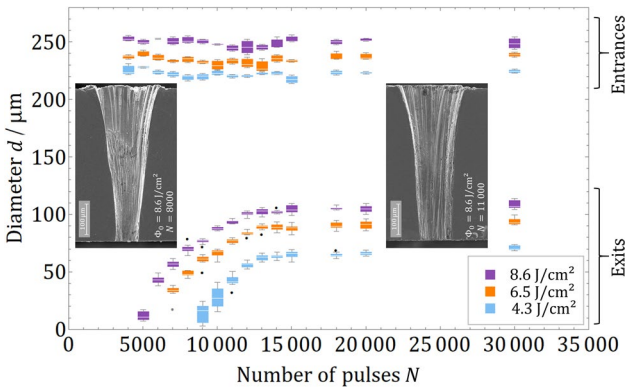

Fig. 5 Development of the mid-range diameter of the exits and the entrances of the microholes which were produced in 0.5 mm thick samples of stainless steel (St 1.4301/AISI 304) with a peak fluence of 8.6 J/cm^2 (violet), 6.5 J/cm^2 (orange) and 4.3 J/cm^2 (blue) in Gaussian beam ($\lambda = 800$ nm,$\tau = 1$ ps,$f_R = 1$ kHz). The insets show the cross section of microholes which were produced with a with a peak fluence of 8.6 J/cm^2 and 8000 pulses (left) and 11,000 pulses (right)

$$A_{\text{cone}} = \pi r_{\text{entr}} \left(r_{\text{entr}}^2 + z_{\text{tip}}^2 \right)^{1/2} \tag{4}$$

is the area of the lateral surface of the conically shaped hole (see Fig. 6b) and, as an amendment to the expression given in [18], we here take into account that only the fraction

$$\frac{1}{E_P} \int_0^{2\pi} \int_0^{r_{\text{entr}}} \Phi(r) r \, dr d\varphi = \left(1 - \frac{\phi_{\text{abs,th}}}{A \, \phi_0} \right) \tag{5}$$

of the pulse energy is incident inside the entrance opening of the hole.

In order to apply this model to the discussion of through-holes, it is assumed that the hole within the workpiece with thickness z_M evolves the same way as if the workpiece was thicker than z_{tip} also when $z_{\text{tip}} > z_M$. This implies that multiple reflections on the walls of the hole do not constitute a significant transport of radiation from the lowest part ($z \in [z_M, z_{\text{tip}}]$) back towards the upper part ($z \in [0, z_M]$) of the cone and that the radiation absorbed on the lower part approximately corresponds to the one that is transmitted through the opening at $z = z_M$ in the case of the through-hole. As seen from the good agreement with the experimental results discussed in Sect. 5, this appears to be a valid first-order assumption despite the strong simplification. The

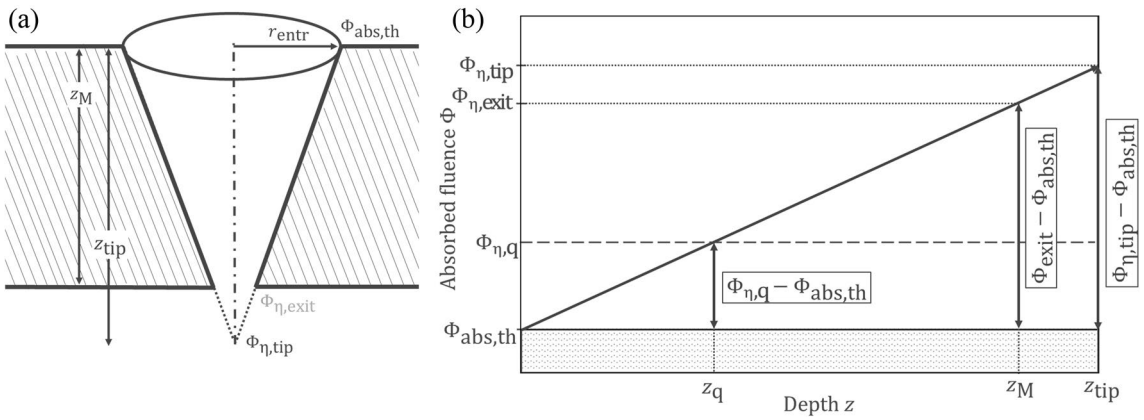

Fig. 6 **a** Conical geometry of the considered microholes. At the edge of the microhole's entrance the fluence is assumed to correspond to the ablation threshold and at the tip of the cone the fluence is $\Phi_{\eta,tip}$ following the model of [18] as shown by (**b**)

absorptance η used for our calculation is thus the one of the complete cone, which was originally introduced by Gouffé [28], with minor corrections by Hügel and Graf [27]

$$\eta = \frac{1 + (1 - A)\left(S_G - \frac{\Omega_G}{2\pi}\right)}{A\left(1 - S_G\right) + S_G}, \tag{6}$$

where S_G represents the ratio between the opening of the microhole and the complete surface area of the cone including the opening and Ω_G is the solid angle under which the aperture is seen from the tip of the hole. For a conical geometry, S_G is given by

$$S_G = 1/\left(1 + \sqrt{1 + \frac{z_{tip}^2}{r_{entr}^2}}\right) \tag{7}$$

and Ω_G is given by

$$\Omega_G = 4\pi \sin^2\left(\frac{1}{2}\arctan\left(\frac{r_{entr}}{z_{tip}}\right)\right). \tag{8}$$

The incremental increase of

$$z_{tip}(N) = z_{tip}(N-1) + z_{abl}(N) \tag{9}$$

provoked by the Nth laser pulse is given by

$$z_{abl}(N) = l_{ep} \ln\left(\frac{\Phi_{\eta,tip}(N)}{\Phi_{abs,th}}\right), \quad \Phi_{\eta,tip} \geq \Phi_{abs,th}, \tag{10}$$

as long as the fluence $\Phi_{\eta,tip}$ absorbed at the tip exceeds the ablation threshold $\Phi_{abs,th}$, where l_{ep} is the effective penetration depth and $f(N)$ denotes the respective quantities as given by the geometry of the hole after N laser pulses with $z_{tip}(0) = 0$ [18].

With the above assumptions and the linear increase of the fluence inside the hole as shown in Fig. 6b, the fluence of the Nth pulse at the depth $z_M \leq z_{tip}(N)$ is found to be

$$\Phi_{\eta,exit}(N) = \frac{z_M}{z_{tip}(N)}\left(\Phi_{\eta,tip}(N) - \Phi_{abs,th}\right) + \Phi_{abs,th}. \tag{11}$$

4.2 Fluence limit for high-quality microhole exits

In view of the hypothesis, that a minimum fluence $\Phi_{\eta,q}$ is required to obtain exits of high quality we further need to calculate at what depth z_q the fluence of the Nth pulse equals $\Phi_{\eta,q}$. As seen from Fig. 6b, this depth is given by

$$z_q(N) = \frac{\Phi_{\eta,q} - \Phi_{abs,th}}{\Phi_{\eta,tip}(N) - \Phi_{abs,th}} z_{tip}(N), \Phi_{\eta,tip} > \Phi_{abs,th}. \tag{12}$$

After breakthrough, the fluence $\Phi_{\eta,exit}(N)$ at the exit of the hole exceeds the value of $\Phi_{\eta,q}$ as long as $z_q(N) \leq z_M$. According to the hypothesis, the quality of the holes therefore is expected to deteriorate as soon as $z_q(N) > z_M$. According to this model, z_q is the depth to which the striations reach into the hole and marks the transition from a corrugated drilling channel to the one with a smooth surface as seen from the left inset of Fig. 5.

Let N^* be the number of pulses at which the tip breaks through the material with the thickness z_M, hence

$$z_{tip}(N^*) = z_M, \tag{13}$$

and N^{**} the number of pulses at which $\Phi_{\eta,exit}$ falls below $\Phi_{\eta,q}$, hence

$$z_q(N^{**}) = z_M. \tag{14}$$

The maximum number of pulses $\Delta N_q = N^{**} - N^*$ that can be applied after breakthrough before the fluence $\Phi_{\eta,\mathrm{exit}}$ falls below $\Phi_{\eta,q}$ is found by solving Eqs. (13) and (14) for N using the Eq. (1) through (12). Due to the implicit formulation of the equations, the solution needs to be performed iteratively. To this end, Eq. (9) may be interpreted as a differential equation

$$\frac{\mathrm{d}z_{\mathrm{tip}}(N)}{\mathrm{d}N} = z_{\mathrm{abl}}\big(z_{\mathrm{tip}}(N), N\big), \quad z_{\mathrm{tip}}(0) = 0, \tag{15}$$

in order to take advantage of corresponding numerical solvers.

5 Experimental verification

Figure 7 shows the experimentally determined values of ΔN_q (black dots) from Sect. 3 as a function of the peak fluence Φ_0 (lower abscissa) or the pulse energy E_P (upper abscissa) of the incident Gaussian beam together with the calculated values of ΔN_q with $\Phi_{\eta,q} = (2.8 \pm 0.2)\,\Phi_{\mathrm{abs,th}}$. The material-specific and laser-specific parameters used for the calculation are listed in Table 1. According to [18], the ablation threshold Φ_{th} corresponds to the single-pulse ablation threshold of iron [29] and AISI 304 [30], so that $\Phi_{\mathrm{abs,th}} = A \bullet \Phi_{\mathrm{th}} = 0.128\ \mathrm{J/cm^2}$. The effective penetration was set to a value of 35 nm [31]. The parameter $\Phi_{\eta,q}$ was estimated by a least squares method. Figure 7 shows that the model with $\Phi_{\eta,q} = 2.8\,\Phi_{\mathrm{abs,th}}$ (=0.36J/cm^2) describes the basic course of the experimental data. According to the model, the formation of striations can be explained by the fact that after ΔN_q pulses the fluence at the edge of the microhole's exit falls below a limit value of $\Phi_{\eta,q} = 2.8\,\Phi_{\mathrm{abs,th}}$.

Figure 7 further reveals that the range, where high-quality exits are formed, can be increased by increasing the peak fluence of the incident Gaussian beam. However, it must be taken into account that when the peak fluence is increased to beyond 10 J/cm^2, intensity-dependent effects such as plasma formation and air breakthrough [32, 33] or heat accumulation effects may occur [13, 34], which can lead to altered ablation and drilling progress.

Taking the criterion $\Phi_{\eta,q} = 2.8\,\Phi_{\mathrm{abs,th}}$ as fluence limit to obtain high-quality exits of the microholes, the evolution of $z_q(N)$ can be determined according to Eq. (12). Figure 8 shows both $z_{\mathrm{tip}}(N)$ (black solid line) and $z_q(N)$ (blue dashed line) as calculated for a peak fluence of 8.6 J/cm^2 in a Gaussian beam with a diameter of 188 µm on the surface of the workpiece at $z = 0$. The horizontal extent of the green unicoloured area at a given depth $z = z_M$ corresponds to the range ΔN_q, in which exits with high quality are expected according to the model assumptions when drilling through a workpiece with the thickness z_M. It reveals that ΔN_q initially increases and then decreases again with increasing depth, so that in this example high-quality exits are only possible up to a material thickness of around 1.2 mm. It should be mentioned that an increasing material thickness leads to an increased aspect ratio, which may influence the material expulsion. This effect is not accounted for in the proposed model.

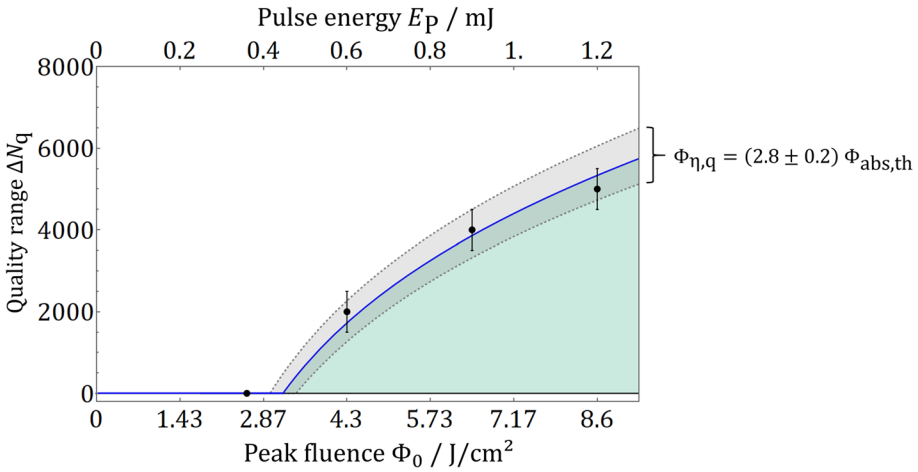

Fig. 7 Number of pulses after breakthrough with high-quality results ΔN_q (black dots) as a function of the peak fluence Φ_0 (lower abscissa) or the pulse energy E_P (upper abscissa) of the incident Gaussian beam with the calculated values of ΔN_q with $\Phi_{\eta,q} = (2.8 \pm 0.2)\,\Phi_{\mathrm{abs,th}}$. The absorbed ablation threshold $\Phi_{\mathrm{abs,th}} = A \bullet \Phi_{\mathrm{th}} = 0.128\ \mathrm{J/cm^2}$ corresponds to the single-pulse ablation threshold of iron and AISI 304. The green area highlights the range ΔN_q of pulses after breakthrough in which high-quality exits are expected according to the model assumptions

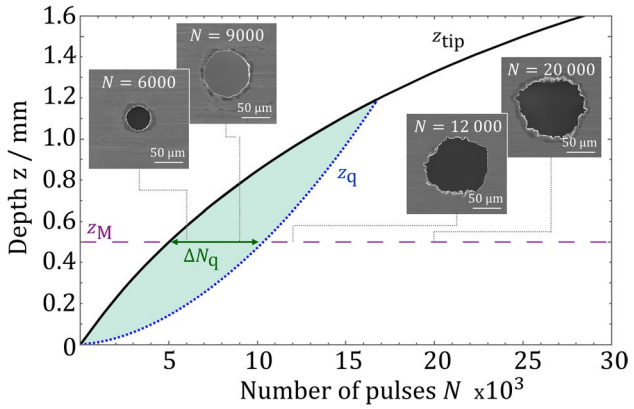

Fig. 8 Progression of z_{tip} (black solid line) according to Eq. (15) and z_q (blue dashed line) according to Eq. (12) for a quality limit fluence of $\Phi_{\eta,q} = 2.8\,\Phi_{abs,th}$ as a function of the number of pulses N for a peak fluence of 8.6 J/cm^2 in Gaussian beam with a diameter of 188 µm at $z = 0$ (St 1.4301/ AISI 304, $\lambda = 800$ nm, $\tau = 1$ ps, $f_R = 1$ kHz, $E_P = 1.2$ mJ). The horizontal extent of the green unicoloured area at a given depth $z = z_M$ corresponds to the range ΔN_q, in which exits with high quality are expected according to the model assumptions, in this figure exemplary shown for $z_M = 0.5$ mm

Table 1 Material-specific parameters for iron and laser-specific parameters used for the model calculation

Model parameter		Value
Absorptivity[a]	A	0.44
Single-pulse ablation threshold[b]	Φ_{th}	0.29 J/cm^2
Beam diameter at $z = 0$	d_s	188 µm
Material thickness	z_M	0.5 mm
Effective penetration depth[c]	l_{ep}	35 nm
Absorbed quality limit fluence (fit parameter)	$\Phi_{\eta,q}$	0.36 J/cm^2

[a] [35], [b][29, 30], [c][31]

6 Conclusion

By comparing results from an experimental study in stainless steel to calculations based on a model for the distribution of the absorbed fluence in conically shaped holes, it was shown that the edge quality of the exit of percussion-drilled microholes strongly depends on the fluence that is absorbed at this location. It was found that the quality of the hole's exit quickly deteriorates with increasing number of pulses as soon as the fluence that is absorbed near the edge of the exit falls below a limit value of 2.8 times the ablation threshold. The number of pulses that can be applied after breakthrough until the quality starts to deteriorate can be increased by increasing the peak fluence of the applied Gaussian beam. The success of common process strategies for the production of high-quality microholes, such as helical drilling and dynamic focus adjustment, might therefore be explained by a significant increase of fluence that is absorbed near the microhole's exit.

Acknowledgements The author would like to thank LightPulse LASER PRECISION and FRAMA GmbH for providing the microscope, Johannes Wahl and Liane Hoster for taking the SEM images and preparing the cross sections, and Jan Winter for the helpful communication and sharing scientific data.

Funding Open Access funding enabled and organized by Projekt DEAL. This work was supported by: Federal Ministry for Economic Affairs and Energy (BMWi) on the basis of a decision by the German Bundestag (contract number ZF4592402FH8) and funded by the Deutsche Forschungsgemeinschaft (DFG, German Research Foundation) – INST 41/1031–1 FUGG.

Declaration

Conflict of interest The authors declare no conflicts of interest.

References

1. T. V. Kononenko, S. M. Klimentov, S. V. Garnov, V. I. Konov, D. Breitling, C. Foehl, A. Ruf, J. Radtke, and F. Dausinger, Hole formation process in laser deep drilling with short and ultrashort pulses. Proc. SPIE 4426. *Second International Symposium on Laser Precision Microfabrication*, p. 108 (25 February 2002)
2. S. Tatra, R.G. Vázquez, C. Stiglbrunner, A. Otto, Numerical simulation of laser ablation with short and ultra-short pulses for metals and semiconductors. Phys. Procedia **83**, 1339–1346 (2016)
3. M. Kraus, D. Walter, A. Michalowski, J. König, Processing techniques and system technology for precise and productive microdrilling in metals, in *Ultrashort Pulse Laser Technology*. ed. by F. Schrempel, and F. Dausinger, Laser Sources and Applications, Vol. 195, pp. 201–230 (2016)
4. A. Feuer, C. Kunz, M. Kraus, V. Onuseit, R. Weber, T. Graf, D. Ingildeev, F. Hermanutz, Influence of laser parameters on quality of microholes and process efficiency. in *Laser Applications in Microelectronic and Optoelectronic Manufacturing (LAMOM) XIX*, SPIE Proceedings (SPIE, 2014), 89670H
5. M. Kraus, M.A. Ahmed, A. Michalowski, A. Voss, R. Weber, T. Graf, Microdrilling in steel using ultrashort pulsed laser beams with radial and azimuthal polarization. Opt. Express **18**, 22305–22313 (2010)

6. A. Michalowski, Melt dynamics and hole formation during drilling with ultrashort pulses. JLMN **3**, 211–215 (2008)
7. M. Henn, G. Reichardt, R. Weber, T. Graf, and M. Liewald, Advances in Dry Metal Forming Using Volatile Lubricants Injected Through Laser-Drilled Microholes. in *Tms 2020 149th annual meeting & exhibition supplem ental proceedings* (Springer Nature, 2020), pp. 1979–1991
8. J.-P. Negel, A. Loescher, D. Bauer, D. Sutter, A. Killi, M. A. Ahmed, T. Graf, Second Generation Thin-Disk Multipass Amplifier Delivering Picosecond Pulses with 2 kW of Average Output Power. in *Advanced Solid State Lasers. Part of Lasers: 30 October-3 November 2016, Boston, Massachusetts, United States*, OSA technical digest (online) (OSA - The Optical Society, 2016), ATu4A.5
9. C. Teisset, C. Wandt, M. Schultze, S. Klingebiel, M. Häfner, S. Prinz, S. Stark, C. Grebing, J.-P. Negel, H. Höck, M. Scharun, T. Dietz, D. Bauer, A. Budnicki, C. Stolzenburg, D. Sutter, A. Killi, T. Metzger, Multi-kW Thin-Disk Amplifiers. In *Mid-Infrared Coherent Sources. Part of High-Brightness Sources and Light-Driven Interactions: 26–28 March 2018, Strasbourg, France*, OSA technical digest (online) (OSA - The Optical Society, 2018), HT1A.6
10. R. Weber, T. Graf, P. Berger, V. Onuseit, M. Wiedenmann, C. Freitag, A. Feuer, Heat accumulation during pulsed laser materials processing. Opt. Express **22**, 11312–11324 (2014)
11. J. Finger, M. Reininghaus, Effect of pulse to pulse interactions on ultra-short pulse laser drilling of steel with repetition rates up to 10 MHz. Opt. Express **22**, 18790–18799 (2014)
12. F. Bauer, A. Michalowski, T. Kiedrowski, S. Nolte, Heat accumulation in ultra-short pulsed scanning laser ablation of metals. Opt. Express **23**, 1035–1043 (2015)
13. R. Weber, T. Graf, C. Freitag, A. Feuer, T. Kononenko, V.I. Konov, Processing constraints resulting from heat accumulation during pulsed and repetitive laser materials processing. Opt. Express **25**, 3966–3979 (2017)
14. D. J. Förster, R. Weber, T. Graf, Residual heat during ultrashort laser drilling of metals. in *Proceedings of LPM2017 - the 18th International Symposium on Laser Precision Microfabrication* (2017)
15. D. Haasler, J. Finger, Investigation of heat accumulation effects during deep hole percussion drilling by high power ultrashort pulsed laser radiation. J. Laser Appl. **31**, 22201 (2019)
16. D.J. Förster, R. Weber, D. Holder, T. Graf, Estimation of the depth limit for percussion drilling with picosecond laser pulses. Opt. Express **26**, 11546–11552 (2018)
17. A. Feuer, D. J. Förster, R. Weber, T. Graf, Depth and quality limit for percussion drilled microholes with depth > 1 mm using ultrashort pulsed laser radiation. in *Proceedings of Lasers in Manufacturing 2019* (2019)
18. D. Holder, R. Weber, T. Graf, V. Onuseit, D. Brinkmeier, D. J. Förster, A. Feuer, Analytical model for the depth progress of percussion drilling with ultrashort laser pulses. Appl. Phys. A **127** (2021)
19. L. Romoli, G. Lovicu, C. Rashed, G. Dini, M. de Sanctis, M. Fiaschi, Microstructural changes induced by ultrashort pulsed lasers in microdrilling of fuel nozzles. Procedia CIRP **33**, 508–513 (2015)
20. F. Hermanutz, D. Ingildeev, M.R. Buchmeiser, A. Feuer, V. Onuseit, R. Weber, New supermicro fibers based on cellulose and cellulose-2.5-acetate. Chem. Fibers Int. **2**, 84–86 (2013)
21. S. Döring, S. Richter, A. Tünnermann, S. Nolte, Evolution of hole depth and shape in ultrashort pulse deep drilling in silicon. Appl. Phys. A Mater. Sci. Process. **105**, 69–74 (2011)
22. S.J. Russell, Artificial intelligence. A modern approach. 3rd, Global ed. (Pearson, 2016)
23. S.B. Kotsiantis, Supervised Machine Learning: A Review of Classification Techniques. in *Emerging artificial intelligence applications in computer engineering. Real word AI systems with applications in eHealth, HCI, information retrieval and pervasive technologies*, ed. by I.G. Maglogiannis (IOS Press, 2007), pp. 3–24
24. L. Morissette, S. Chartier, The k-means clustering technique: General considerations and implementation in Mathematica. TQMP **9**, 15–24 (2013)
25. J.M. Liu, Simple technique for measurements of pulsed Gaussian-beam spot sizes. Opt. Lett. **7**, 196–198 (1982)
26. J. Furmanski, A.M. Rubenchik, M.D. Shirk, B.C. Stuart, Deterministic processing of alumina with ultrashort laser pulses. J. Appl. Phys. **102**, 73112 (2007)
27. H. Hügel, T. Graf, *Laser in der Fertigung. Grundlagen der Strahlquellen, Systeme, Fertigungsverfahren*, 3., überarb. und erw. Aufl. (Springer Vieweg, 2014)
28. A. Gouffé, Correction d'ouverture des corps-noirs artificiels compte tenu eds diffusions multiples internes. Revue d'Optique, 1–10 (1945)
29. I.A. Artyukov, D.A. Zayarniy, A.A. Ionin, S.I. Kudryashov, S.V. Makarov, P.N. Saltuganov, Relaxation phenomena in electronic and lattice subsystems on iron surface during its ablation by ultrashort laser pulses. Jetp Lett. **99**, 51–55 (2014)
30. J. Winter, M. Spellauge, J. Hermann, C. Eulenkamp, H.P. Huber, M. Schmidt, Ultrashort single-pulse laser ablation of stainless steel, aluminium, copper and its dependence on the pulse duration. Opt. Express **29**, 14561 (2021)
31. J. Winter, Additional data set for 1 ps following [30]. In these data, the effective penetration depth for fluences of is 35 nm (AISI 304, 1056nm). (personal communication, 2021)
32. S.M. Klimentov, T.V. Kononenko, P.A. Pivovarov, S.V. Garnov, V.I. Konov, A.M. Prokhorov, D. Breitling, F. Dausinger, The role of plasma in ablation of materials by ultrashort laser pulses. Quantum Electron. **31**, 378–382 (2001)
33. S.M. Klimentov, S.V. Garnov, V.I. Konov, T.V. Kononenko, P.A. Pivovarov, O.G. Tsarkova, D. Breitling, F. Dausinger, Effect of low-threshold air breakdown on material ablation by short laser pulses. Phys. Wave Phen. **15**, 1–11 (2007)
34. T.V. Kononenko, C. Freitag, D.N. Sovyk, A.B. Lukhter, K.V. Skvortsov, V.I. Konov, Influence of pulse repetition rate on percussion drilling of Ti-based alloy by picosecond laser pulses. Opt. Lasers Eng. **103**, 65–70 (2018)
35. P. Johnson, R. Christy, Optical constants of transition metals: Ti, V, Cr, Mn, Fe Co, Ni, and Pd. Phys. Rev. B **9**, 5056–5070 (1974)